EUROFUSION CP(15)04/30

G. Meisl et al.

# Simulating the Nitrogen Migration in Be/W Tokamaks with WallDYN

(18th May 2015 – 22nd May 2015)
Aix-en-Provence, France

# Simulating the nitrogen migration in Be/W tokamaks with WallDYN

**G. Meisl**[a], **K. Schmid**[a], **K. Krieger**[a,b], **M. Oberkofler**[a], **S.W. Lisgo**[c] **and JET contributors**[b]

[a] **Max-Planck-Institut für Plasmaphysik, Boltzmannstraße 2, 85748 Garching, Germany**

[b] **EUROfusion Consortium, JET, Culham Science Centre, OX14 3DB, Abingdon, UK** ‡

[c] **ITER Organization, FST, Route de Vinon, CS 90 046, 13067 Saint Paul Lez Durance Cedex, France**

E-mail: `gmeisl@ipp.mpg.de`

**Abstract.**

The migration of wall material or seeding impurities plays an important role in the formation of mixed materials, the impurity contamination of the plasma and tritium retention. First, this work presents an improved model for the sputtering from mixed material surfaces in WallDYN. Second, we present dynamic SDTrimSP and WallDYN simulations of the nitrogen implantation in Be and the migration of nitrogen in tokamaks

---

‡ See the Appendix of F. Romanelli et al., Proceedings of the 25th IAEA Fusion Energy Conference 2014, Saint Petersburg, Russia

with Be main wall. The simulations with the binary collision code SDTrimSP predict that N accumulates directly at the surface and that the Be erosion decreases with increasing N surface content. A first application of WallDYN to the nitrogen migration with ITER-like wall indicates that the Be main wall may cause wall pumping of N by co-deposition with Be.

PACS numbers: 79.20.Ap, 52.25.Vy, 52.40.Hf, 52.65.-y

## 1. Introduction

Experiments in ASDEX Upgrade (AUG) and JET have demonstrated the ability to control the power load onto the divertor target plates by $N_2$ puffing [1, 2, 3]. In contrast to hydrogen and noble gases, N chemically interacts with tungsten and beryllium surfaces. This leads to a storage of nitrogen from the plasma in the wall surfaces. As the surfaces have only a limited N storage capacity, excess N is reemitted from saturated surfaces.

The accumulation and migration of N in tokamaks has already been studied experimentally in AUG [4, 5, 6, 7, 8], TEXTOR [9] and JET [10, 11, 12]. For AUG many of the experimental results could be reproduced by WallDYN simulations employing a novel model for the N saturation [7, 8].

This work employs WallDYN to study the impact of the Be main wall in JET and ITER on the N migration. As a first step, the accumulation of N in Be under D-N co-bombardment is studied with SDTrimSP simulations [13]. Then, recent extensions to the WallDYN model are described which improve the accuracy of the sputter and N-saturation models. Finally, WallDYN predictions on the N accumulation in JET-ILW and ITER are presented. It has to be pointed out, that these simulations cannot yet give a concluding picture of the N migration in JET or ITER, but rather should help to prepare experiments for a detailed benchmarking of WallDYN.

Currently, only few experimental results concerning the N migration in JET-ILW are available: A study of the N retention and legacy with Be main wall, mainly based on residual gas analysis and spectroscopy, was reported in Ref. [11]. A surface analysis of tiles removed from JET reported a rather inhomogeneous distribution of N, with a pronounced maximum in the net-deposition region on the apron above the inner divertor [12].

## 2. Accumulation of N in Be under D-N co-bombardment

SDTrimSP [13] is widely used to simulate the interaction of energetic ions with matter. It is based on the binary collision approximation in combination with electronic stopping, so that chemical effects are not readily taken into account. However, earlier studies have shown that SDTrimSP with a maximum N concentration for N in Be of 40 % is well suited for the simulation of N implantation in Be [14, 15]. As for the case of W-surfaces in Ref. [16], the accumulation of N in Be under bombarded with D and N atoms with an impact angle of 40° and $E_N = 2E_D$ has been simulated with SDTrimSP for varying energies ($E$) and N fraction in the beam. It should be noted that SDTrimSP and the present discussion do not include diffusive or chemical effects, so the simulations are valid only at low temperatures. The decomposition of beryllium nitride seems only to set in above 1000 K [14]. However, the formation of tungsten nitride is suppressed already at significantly lower temperatures [16]. Temperature effects could be important especially for ITER, where divertor surface temperatures above 1000 K are expected.

Figure 1 shows exemplarily the N depth profiles arising from bombarding a Be surface with 92 % D and 8 % N. With increasing energy the implantation depth and the N content increase. Different from the case of W surfaces with a N peak in a few nm depth [16], the maximum N concentration develops on the surface. Furthermore, simulations on the bombardment of Be surfaces with a mixture of D+N+Be (not shown here) indicate that the N/Be ratio in deposited layers does not reach the ratio of stoichiometric $Be_3N_2$.

Figure 2 shows that for all considered impact conditions the N saturation areal density increases with increasing implantation energy. With increasing D fraction in the beam the N areal density decreases, because the D leads to an enhanced N re-erosion. Figure 1 also includes results from the WallDYN model, which are discussed in section 3. In this section also sputtering of Be under D-N bombardment is discussed. It should be noted that the sputter and reflection yield in WallDYN are calculated from fits to static SDTrimSP calculations. Still, deviations between WallDYN and SDTrimSP can arise from depth profile effects, as WallDYN assumes a homogeneous composition of the surface.

## 3. WallDYN model and recent improvements

To include the complete migration chain of erosion, transport through the plasma, re-deposition and potential re-erosion in our analysis, we employ the WallDYN code [8, 17] for our analysis of the N migration. WallDYN simulates the evolution of the surface composition of the first wall, which is discretized into about 50 poloidally distributed wall tiles. The plasma-wall interaction module of WallDYN includes physical sputtering and reflection based on SDTrimSP calculations. The transport of impurities in the plasma is calculated with DIVIMP [18]. An important input for WallDYN and DIVIMP is the plasma background, i.e. spatially resolved data on the plasma density, temperature and flow velocity.

The plasma background employed for the ITER simulations is based on a SOLPS simulation of a medium density H-mode ($P_{SOL}$=100 MW) plasma. As shown in Fig. 4 the SOL flows are rather weak. To improve the accuracy of the plasma-wall interaction in the main wall region, the plasma was extrapolated from the SOLPS grid to the main wall with the onion-skin model as described in Ref. [19]. For the JET simulations the plasma background for the ohmic shot of Ref. [20] was employed. For the perpendicular transport of impurities a constant anomalous diffusion coefficient of $D_\perp = 1$ $m^2s^{-1}$ was used. It should be noted, that the plasma backgrounds do not include the effect of nitrogen seeding on the plasma. The JET OSM solution represents a pure D plasma, the SOLPS plasma for ITER consists of D as main species and small amounts of He and C.

The loss of N to the vacuum pumping system is modeled by pumping tiles (green lines in Fig. 4) with zero sputter and reflection yield. As described in Ref. [8], a model to reproduce the N saturation in W has recently been included in WallDYN. For the present work, this model was extended to include the energy dependence of the N saturation areal density ($\sigma_{Sat}$) in Be. Based on the SDTrimSP simulations presented in the previous section the employed N saturation areal density is:

$$\sigma_{Sat} = \left(0.25 + 0.003 \cdot \frac{2\,T_i + 2\,T_e}{\mathrm{eV}}\right) 10^{20}\,\mathrm{N/m^2} \qquad (1)$$

Figure 2 gives a direct comparison of SDTrimSP simulations to results from WallDYN. It should be noted that the reflection and sputter yields in WallDYN are calculated from fits to static SDTrimSP simulations. Still, deviations between SDTrimSP and WallDYN arise because WallDYN does not take into account the effects arising from the elemental depth distribution. The dark green dotted curve is based on the WallDYN surface model without a maximum areal density. In contradiction to the experimental results the N areal density rises continuously. The WallDYN results using the energy dependent $\sigma_{Sat}$ (dotted and dashed curves) largely agree with SDTrimSP. The only notable exception is the WallDYN simulation for 3 % N and $E_D$=250 eV. While there is a slight decrease in the saturation N areal density with decreasing N fraction in all WallDYN simulations, the strong N re-erosion for this special case is not reproduced by WallDYN. The reason for this discrepancy is the assumption of a homogeneous surface layer in WallDYN. Because the real N depth profile is peaked towards the surface, the real N re-erosion is higher than predicted by WallDYN§.

It should be noted that the WallDYN N saturation model only limits the N content of the reaction zone [17]. The total N areal density may rise above the given limit due to co-deposition with other species. In this case, the concentration of N in the co-deposits is given by the maximum concentration resulting from (1). For the present WallDYN simulations the resulting N/Be ratio lies (incidentally) in the range reported from PISCES-B experiments [11, 22].

### *3.1. Sputtering of mixed materials*

As described in Ref. [17] the sputter yield of species $e$ from a mixed material surface in WallDYN is usually calculated by

$$Y^{e}_{sput} = \frac{\sigma_e}{\sigma_{tot}} \cdot Q_0 \cdot Y_{Bohdansky}(E_{Kin}, E_{Thresh}) \cdot \left(1 + \sum_{i=1}^{N} a_i \sigma_i\right) \tag{2}$$

where $E_{Kin}$ is the kinetic energy of the impinging particle, $\sigma_i$ is the areal density and $\sigma_i/\sigma_{tot}$ the concentration of species $i$ in the target surface, $N$ the number of elements, and the parameters $Q_0$, $E_{Threshold}$ and $a_i$ are determined individually for each projectile-target combination by a fit to SDTrimSP simulations. This formula works well in that it generally reproduces the known energy dependence of the sputter yield and includes effects of the composition on the sputter yield. A technical problem related to this formula is the interdependency of the parameters $Q_0$ and $a_e$. This makes it rather difficult to compare different sets of these parameters or to compare such parameters to experimental results.

§ For N in W it is just the other way round and WallDYN seems to overestimate the N erosion [8]

To overcome this problem a modified expression for the sputter yield was introduced in WallDYN:

$$Y^{e}_{sput} = \frac{\sigma_e}{\sigma_{tot}} \cdot Q_0^{pure} \cdot Y_{Bohdansky}(E_{Kin}, \tilde{E}_{Thresh}) \cdot \left(1 + a_e\left(1 - \frac{\sigma_e}{\sigma_{tot}}\right)\right) \cdot \prod_{i \neq e}^{N} \left(1 + a_i \frac{\sigma_i}{\sigma_{tot}}\right); \quad a_i > -1 \tag{3}$$

where $Q_0^{pure}$ is fitted to SDTrimSP simulations with $\sigma_e/\sigma_{tot} = 1$ and can be easily compared to experimental results. A composition dependence is introduced by the terms $a_i$ and by $\tilde{E}_{Threshold}$

$$\tilde{E}_{Thresh} = E^{pure}_{Thresh} \cdot \left(1 + b_e\left(1 - \frac{\sigma_e}{\sigma_{tot}}\right)\right) \cdot \prod_{i \neq e}^{N} \left(1 + b_i \frac{\sigma_i}{\sigma_{tot}}\right); \qquad b_i > -1 \tag{4}$$

which is composed of $E^{pure}_{Threshold}$, the threshold energy for a pure elemental surface with $\sigma_e/\sigma_{tot} = 1$, and a term representing the composition dependence of the threshold energy. This model for the sputtering from mixed surfaces avoids the problems associated with the interdependency of $Q_0$ and $a_e$, but also results in a better quality of the fits.

Figure 3 shows the evolution of the Be sputter yield under D-N bombardment from SDTrimSP and WallDYN simulations. The sputter yields for pure Be agree very well. Also both codes predict a decrease of the Be sputter yield due to N accumulation in the surface‖. The magnitude of this decline depends on the enrichment of N at the surface, and is therefore smaller in WallDYN than in SDTrimSP.

---

‖ In contrast, SDTrimSP predicts that the W sputter yield under D-N bombardment is constant [16]

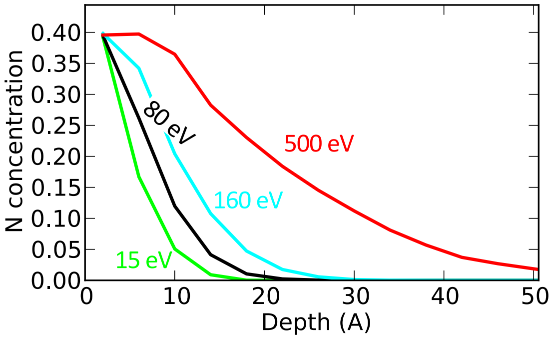

**Figure 1.** Steady state N depth profiles in a Be surface under bombardment with D and 8 %N, $E_N$=2 $E_D$.

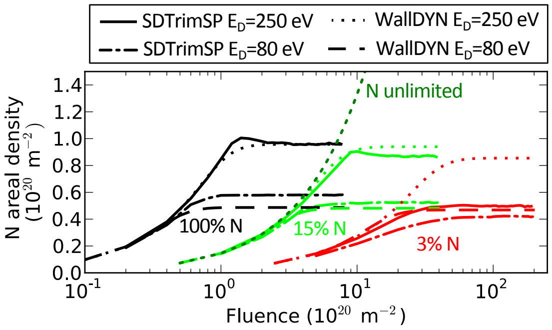

**Figure 2.** Accumulation of N in Be surface under D-N bombardment calculated with SDTrimSP and the WallDYN model. N has twice the energy of D. The color indicates the fraction of N in the incoming beam. For 15 % N also a simulation with the WallDYN model without saturation model is shown. The N areal density increases with increasing energy and increasing N fraction.

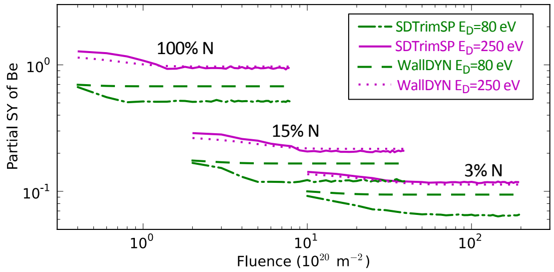

**Figure 3.** Partial sputter yield evolution of Be under D-N bombardment with $E_N = 2E_D$ calculated with SDTrimSP and WallDYN.

## 4. Application of WallDYN to the N migration in tokamaks with Be main wall

Similar to the WallDYN predictions for AUG, N starts to accumulate in the surfaces close to the injection location and in the divertor. The N areal density predicted for 15 s with the ITER geometry and a N puff of $1.43 \cdot 10^{22} \frac{\mathrm{N}}{\mathrm{s}}$ ¶ from the divertor is shown in Fig. 4. One can see that N is present in the whole divertor region and in large parts of the main wall. The dark areas of the wall represent regions, where the N areal density significantly exceeds the N saturation areal density specified for the reaction zone. These areas are regions of net Be deposition and the comparatively high N areal densities result from a "co-deposition" of N with Be. SOL flows to the high field side, as they are usually observed experimentally [21], would shift the Be deposition areas, and therefore the N co-deposition, to the high field side.

This is actually the case for the JET simulations, which are based on a plasma background featuring strong SOL flows towards the high field side. In these simulations the co-deposition of N with Be is predicted to occur on the apron above the inner divertor, similar to the results from Ref. [12]. For the long term N balance the co-deposition of N with Be leads to a continuous increase of the N wall inventory, different from the case of AUG with a W main wall. As an estimate for the wall inventory in JET after puffing $3.8 \cdot 10^{22}$ N atoms the simulation gives a value of $0.9 \cdot 10^{22}$ N atoms. This value

¶ Corresponding to a very strong N puff in JET has to be compared to $2 \cdot 10^{22}$ N atoms, which were missing in the gas balance in Ref. [11]. Taking into account that part of the missing N probably sticks in the vessel in the form of ammonia (a process not included in WallDYN) and the uncertainties entering the calculation of this number, this seems like a reasonable agreement.

Finally, we want to discuss the impact of the plasma wall interaction on the N fluxes and distribution in the plasma. To this end Fig. 5 shows the results from 4 WallDYN simulations with ITER geometry. These simulations differ in the location of the N puff, which is either in the divertor or from the vessel top, and in the magnitude of the sputter and reflection yields, which are based either on simulations with perpendicular impact or an impact angle of 40°. In Fig. 5a one can see the evolution of the effective N flux into the plasma. The initial flux is only somewhat above the puff rate of $1.43 \cdot 10^{22} \frac{\mathrm{N}}{\mathrm{s}}$. As the surfaces get saturated with N, the effective N reflection coefficient and the N flux into the plasma rise. Thereby the N flux is higher for a puff from the vessel top (further away from the pumping system) and lower for the simulations with higher sputter yield (which leads to stronger wall pumping by co-deposition). Figure 5b shows the ratio of N fluxes in the divertor to the N core concentration as a measure for the divertor enrichment. For the N puff from the vessel top the wall pumping reduces the divertor enrichment and so the saturation of the surface N content increases the divertor enrichment. For the N puff from the divertor, less N is transported into the main plasma with stronger wall pumping. That means the divertor enrichment goes down with increasing N surface coverage or smaller sputter yields. However, the WallDYN predicts an increased divertor enrichment for the case of a divertor puff.

## 5. Conclusion

This work is part of an effort to improve the understanding of N migration by combining laboratory experiments, computer simulations and tokamak experiments [7, 8, 16]. The present contribution extends this study to tokamaks with a Be main wall. To get a better insight into the interaction of energetic N with a plasma exposed Be surface, SDTrimSP simulations have been performed. These simulations result in N depth profiles, where the N concentration steadily decreases with increasing depth and where the N saturation areal density increases with implantation energy. However, as experimental studies on the interaction of N with Be are scarce, significant uncertainties remain, especially with respect to processes like chemical erosion of N from Be [22], the diffusion of N in Be or the co-deposition of N with Be .

Based on the results from SDTrimSP, an energy dependent N saturation areal density has been introduced to describe the interaction of N with Be in WallDYN. Additionally, an improved model for the physical sputtering of mixed material surfaces has been included in WallDYN. According to the WallDYN simulations N becomes stored in the divertor and main wall surfaces and the co-deposition of N with Be may lead to comparatively large N areal densities in net-deposition areas.

## 6. Acknowledgments

This work has been carried out within the framework of the EUROfusion Consortium and has received funding from the Euratom research and training programme 2014-2018 under grant agreement No 633053. The views and opinions expressed herein do not necessarily reflect those of the European Commission. This world was done under EUROFUSION WP PFC.

[1] A. Kallenbach, M. Balden, et al., *J. Nucl. Mater 415, S19 (2011)*, `http://dx.doi.org/10.1016/j.jnucmat.2010.11.105`

[2] F. Reimold, M. Wischmeier, et al., *J. Nucl. Mater. in Press*, `http://dx.doi.org/10.1016/j.jnucmat.2014.12.019`

[3] M. Wischmeier, The ASDEX Upgrade team and JET EFDA contributors, *J. Nucl. Mater. in Press*, `http://dx.doi.org/10.1016/j.jnucmat.2014.12.078`

[4] A. Kallenbach, R. Dux, et al., *Plasma Phys. Control. Fusion 52 055002 (2010)*, `dx.doi.org/10.1088/0741-3335/52/5/055002`

[5] D. Neuwirth, V. Rohde, et al., *Plasma Phys. Control. Fusion 54 085008 (2012)*, `http://dx.doi.org/10.1088/0741-3335/54/8/085008`

[6] P. Petersson, A. Hakola, et al., *J. Nucl. Mater. 438, S616 (2013)*, `http://dx.doi.org/10.1016/j.jnucmat.2013.01.129`

[7] G. Meisl, K. Schmid, et al., *J. Nucl. Mater. (2014), in Press*, `http://dx.doi.org/10.1016/j.jnucmat.2014.10.031`

[8] G. Meisl, K. Schmid, et al., Experimental analysis and WallDYN simulations of the global nitrogen migration in ASDEX Upgrade L-mode discharges, *submitted to Nuclear Fusion*

[9] M. Rubel, V. Philipps, et al. *J. Nucl. Mater. 415, S223 (2011)*, `http://dx.doi.org/10.1016/j.jnucmat.2010.08.035`

[10] S. Brezinsek, T. Loarer, et al., *Nucl. Fusion 51, 073007 (2011)*, `http://dx.doi.org/10.1088/0029-5515/51/7/073007`

[11] M. Oberkofler, D. Douai, et al., *J. Nucl. Mater 438, S258* (2013), `http://dx.doi.org/10.1016/j.jnucmat.2013.01.041`

[12] P. Petersson , M. Rubel, et al., *J. Nucl. Mater., in Press*, `http://dx.doi.org/10.1016/j.jnucmat.2014.12.077`

[13] A. Mutzke, R. Schneider, et al., *IPP Report 12/08, Max-Planck-Institut für Plasmaphysik (Hrsg.) (2011)*

[14] M. Oberkofler, and Ch. Linsmeier, *Nucl. Fusion 50, 125001 (2010)*, `http://dx.doi.org/10.1088/0029-5515/50/12/125001`

[15] K. Dobes, M. Köppen, M. Oberkofler, et al., *NIMB 340, 3438 (2014)*, `http://dx.doi.org/10.1016/j.nimb.2014.06.025`

[16] G. Meisl, K. Schmid, et al., *New J. Phys. 16, 093018 (2014)*, `http://dx.doi.org/10.1088/1367-2630/16/9/093018`

[17] K. Schmid, M. Reinelt, and K. Krieger, *J. Nucl. Mater. 415, S284 (2011)*, `http://dx.doi.org/10.1016/j.jnucmat.2011.01.105`

[18] P.C. Stangeby, J.D. Elder, *J. Nucl. Mater 196, 258 (1992)*, `http://dx.doi.org/10.1016/S0022-3115(06)80042-5`

[19] S.W. Lisgo, A. Kukushkin, et al., *J. Nucl. Mater. 438, S580 (2013)*, `http://dx.doi.org/10.1016/j.jnucmat.2013.01.121`

[20] K. Schmid, K. Krieger, et al., *J. Nucl. Mater., in Press*, `http://dx.doi.org/10.1016/j.jnucmat.2014.11.109`

[21] G.F. Matthew, *J. Nucl. Mater. 337, 1 (2005)*, `http://dx.doi.org/10.1016/j.jnucmat.2004.10.075`

[22] T. Dittmar, M.J. Baldwin, et al., *Phys. Scr. T145, 014009 (2011)*, `http://dx.doi.org/10.1088/`

`0031-8949/2011/T145/014009`

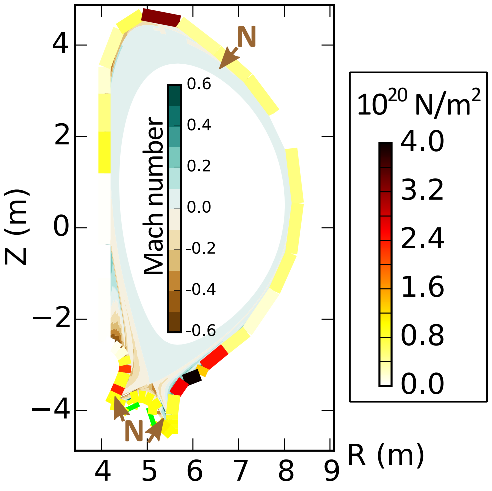

**Figure 4.** N areal density after 15 s for a N puff from the divertor. In net deposition areas the N areal density exceeds the specified saturation areal density. The plasma background exhibits only weak flows in the SOL.

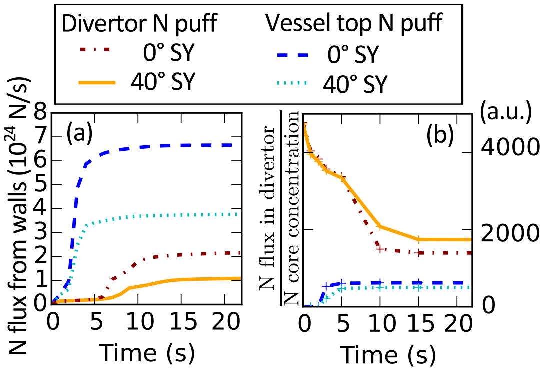

**Figure 5.** Impact of the plasma-wall interaction on N fluxes and distribution in the plasma.